Theoretical Study on the Predissociation Mechanism of CO_2^+ ($C\ ^2\Sigma_g^+$)

Qingyong Meng, Ming-Bao Huang,* and Hai-Bo Chang

College of Chemistry and Chemical Engineering, Graduate University of Chinese Academy of Sciences, P.O. Box 4588, Beijing 100049, People's Republic of China

Received: July 31, 2009; Revised Manuscript Received: September 2, 2009

The main purpose of the present theoretical work was to study predissociation mechanism of the $C\ ^2\Sigma_g^+$ state of the CO_2^+ ion using the CAS methods. Since the $X\ ^2\Pi_g$, $A\ ^2\Pi_u$, $B\ ^2\Sigma_u^+$, $1\ ^4\Sigma_g^-$, and $1\ ^4\Pi_u$ states are involved in the predissociation, we also studied these five states. The CASPT2 calculations indicate that Renner−Teller splitting in $1\ ^4\Pi_u$ leads to two C_{2v} states, $1\ ^4A_1$ and $1\ ^4B_1$. For the $X\ ^2\Pi_g$, $A\ ^2\Pi_u$, $B\ ^2\Sigma_u^+$, and $C\ ^2\Sigma_g^+$ states, the CASPT2 T_0 values and geometries are in good agreement with experiment. The CASPT2 calculations for the O-loss dissociation potential energy curves indicate that the $1\ ^4\Sigma_g^-$, $X\ ^2\Pi_g$, $1\ ^4\Pi_u$, $A\ ^2\Pi_u$, $B\ ^2\Sigma_u^+$, and $C\ ^2\Sigma_g^+$ states correlate with the first, second, second, third, third, and fourth dissociation limits, respectively. The CASSCF minimum energy crossing point (MECP) calculations (in the $C_{\infty v}$, C_s, and C_{2v} symmetries) were performed for selected state/state pairs, and the spin−orbit couplings were calculated at the MECPs. All the MECPs (including the $C\ ^2\Sigma_g^+/1\ ^4\Pi_u$ ($1\ ^4B_1$) MECP), involved in the proposed predissociation mechanism of Praet et al. (*J. Chem. Phys.* **1982**, *77*, 4611−4618), were found and the calculated spin−orbit couplings at these MECPs are not small. Our calculations support the mechanism of Praet et al. and indicate that an energy value of 8.9 eV from CO_2^+ ($X\ ^2\Pi_g$) is needed. The $C\ ^2\Sigma_g^+$ state in the previous [1 + 1] photodissociation experiments (*J. Chem. Phys.* **2008**, *128*, 164308.) could predissociate through the mechanism of Praet et al. since the two-photon energy was around 8.9 eV, while the $C\ ^2\Sigma_g^+$ state in the previous VUV-PFI-PE experiments (*J. Chem. Phys.* **2003**, *118*, 149−163) would predissociate through another mechanism via $A\ ^2\Pi_u$.

1. Introduction

Because the CO_2^+ ion plays an important role in planetary atmospheres,[1] extensive experimental studies on the electronic states,[2−9] vibrational structures,[2−13] and photodissociation mechanisms[5−7,14−20] (in particular the predissociation mechanism of the $C\ ^2\Sigma_g^+$ state) of the CO_2^+ ion were reported in the literature, including photoelectron (PE) measurements,[9−11] vacuum ultraviolet (VUV) pulsed field ionization (PFI)-photoelectron (PFI-PE) measurements,[5−7] and resonance enhanced multiphoton ionization experiments,[17−20] and so forth.

In 1982 Praet et al.[21] reported their theoretical study on the $C\ ^2\Sigma_g^+$ state of CO_2^+ using the LCAO-MO-SCF-CI calculation methods and nonadiabatic reaction theory. On the basis of their calculation results and the previously observed experimental facts, Praet et al.[21] suggested a predissociation mechanism of the $C\ ^2\Sigma_g^+$ state of CO_2^+ which consisted of the following three processes:

$$CO_2^+(C\ ^2\Sigma_g^+) \rightarrow CO_2^+(1\ ^4\Pi_u, \text{repulsive}) \rightarrow O(^3P_g) + CO^+(X\ ^2\Sigma^+) \quad \text{(I)}$$

$$CO_2^+(1\ ^4\Pi_u, \text{repulsive}) \rightarrow 1\ ^4\Pi_u/1\ ^4\Sigma_g^- \text{ conical intersection} \rightarrow CO_2^+(1\ ^4\Sigma_g^-) \rightarrow O^+(^4S_u) + CO(X\ ^1\Sigma^+) \quad \text{(II)}$$

$$CO_2^+(1\ ^4\Sigma_g^-) \rightarrow CO_2^+(X\ ^2\Pi_g) \rightarrow O(^3P_g) + CO^+(X\ ^2\Sigma^+) \quad \text{(III)}$$

Process II starts from the second species in process I and process III starts from the third species in process II.

In 2003 Liu et al.[5] measured the VUV-PFI-PE spectrum of CO_2 in the energy region 19.0−20.0 eV from CO_2 ($X\ ^1\Sigma_g^+$), and they also performed calculations (see below). Liu et al.[5] suggested the same predissociation mechanism for the $C\ ^2\Sigma_g^+$ state as Praet et al.,[21] and they also suggested another predissociation mechanism via the $A\ ^2\Pi_u$ and $1\ ^4\Sigma_g^-$ states described by the following process:

$$CO_2^+(C\ ^2\Sigma_g^+) \rightarrow CO_2^+(A\ ^2\Pi_u) \rightarrow CO_2^+(1\ ^4\Sigma_g^-) \rightarrow O^+(^4S_u) + CO(X\ ^1\Sigma^+) \quad \text{(IV)}$$

In 2008 Yang et al.[20] reported the mass-resolved [1 + 1] two-photon dissociation spectra of the CO_2^+ ion in the wavelength range of 235−354 nm (5.28−3.50 eV). Yang et al.[20] suggested the same predissociation mechanism for the $C\ ^2\Sigma_g^+$ state as Praet et al.[21]

The main purpose of the present theoretical work was to study the predissociation mechanism of the $C\ ^2\Sigma_g^+$ state of the CO_2^+ ion, and in the calculations we used the multiconfiguration

* Corresponding author. Telephone: 86-10-88256129. Fax: 86-10-88256129. E-mail: mbhuang1@gucas.ac.cn.

10.1021/jp907351s CCC: $40.75
Published on Web 10/01/2009

$$O_1-C-O_2$$

Figure 1. Atom labelings for the CO_2^+ ion used in the present work.

second-order perturbation theory (CASPT2)[22,23] method (based on the complete active space self-consistent-field (CASSCF)[24] calculations). Since some other states of CO_2^+ may be involved in the predissociation of the C $^2\Sigma_g^+$ state, we totally calculated six states: X $^2\Pi_g$, A $^2\Pi_u$, B $^2\Sigma_u^+$, C $^2\Sigma_g^+$, 1 $^4\Sigma_g^-$, and 1 $^4\Pi_u$. It is now well-known that CASPT2 and MRCI (internally contracted multireference configuration interaction) methods (both based on CASSCF calculations) are the effective methods for theoretical studies on excited electronic states of small molecules and molecular ions. The calculation methods used by Praet et al.[21] in 1982 were old, but their suggested predissociation mechanism (see above) for the C $^2\Sigma_g^+$ state might be valuable.[5,19,20] Liu et al.[5] calculated electronic states of CO_2^+ using the MRCI method and potential energy curves for some of the states possibly involved in the predissociation of CO_2^+ (C $^2\Sigma_g^+$) using the CASSCF method. We note that their CASSCF potential energy curves (in Figure 8 of ref 5) did not well converge to the dissociation product groups.

After the CASPT2 geometry optimization calculations for the six states of the CO_2^+ ion, we calculated CASPT2 O-loss dissociation potential energy curves (PECs) for the six states. We performed the CASSCF minimum energy crossing point (MECP) calculations for the state/state pairs and calculated the CASSCF spin−orbit coupling values at the MECPs. On the basis of our calculation results, we will examine the predissociation mechanism (consisting of processes I, II, and III) of the C $^2\Sigma_g^+$ state suggested by Praet et al.[21] and discuss the predissociation mechanisms of the C $^2\Sigma_g^+$ state in the experiments of Liu et al.[5] and Yang et al.[20]

2. Calculation Details

Geometry and atom labeling used for the CO_2^+ ion are shown in Figure 1. For the electronic states of the CO_2^+ ion, the calculations were performed in the D_{2h} subgroup of $D_{\infty h}$, where Σ_g^+ corresponds to the A_g irreducible representation, Σ_u^+ to B_{1u}, Σ_g^- to B_{1g}, Π_g to $B_{2g} + B_{3g}$, and Π_u to $B_{2u} + B_{3u}$. In O-loss dissociation process the CO_2^+ system remains in the $C_{\infty v}$ symmetry, and the calculations were performed in the C_{2v} subgroup of $C_{\infty v}$, where Σ^+ corresponds to the A_1 irreducible representation, Σ^- to A_2, and Π to B_1+B_2.

The CAS (CASSCF and CASPT2) calculations[22−24] were carried out using MOLCAS v6.2 quantum-chemistry softwares.[25] A contracted atomic natural orbital (ANO-L) basis set,[26−29] C(5s4p3d2f)/O(5s4p3d2f), was used. With a CASSCF wave function constituting the reference function, the CASPT2 calculations were performed to compute the first-order wave function and the second-order energy in the full-space. In our CAS calculations for the CO_2^+ ion and related species (the CO molecule, the CO^+ and O^+ ions, and the O atom) we always use the full valence active spaces. The HF/6-31G calculations for the ground-state CO_2 molecule produce electron configuration of $(1\sigma_u^+)^2\ (1\sigma_g^+)^2\ (2\sigma_g^+)^2\ (3\sigma_g^+)^2\ (2\sigma_u^+)^2\ (4\sigma_g^+)^2\ (3\sigma_u^+)^2\ (1\pi_u)^4\ (1\pi_g)^4\ (2\pi_u)^0\ (5\sigma_g^+)^0\ (4\sigma_u^+)^0$. For the CO_2^+ ion, 15 electrons were active and the full valence active space included the $3\sigma_g^+-5\sigma_g^+$, $2\sigma_u^+-4\sigma_u^+$, $1\pi_u-2\pi_u$, and $1\pi_g$ orbitals within the $D_{\infty h}$ point group. These active orbitals were labeled within the D_{2h} subgroup in the order A_g, B_{3u}, B_{2u}, B_{1g}, B_{1u}, B_{2g}, B_{3g}, and A_u and the full valence active space is named (32203110). In the calculations for the C_{2v} (denoted as C_{2v}(b); with the C_2-axis bisecting the O_1CO_2 angle; see Figure 1) states of the CO_2^+ ion (due to the Renner−Teller effect or some other reasons), these active orbitals were labeled within the C_{2v} group in the order A_1, B_1, B_2, and A_2 and the full valence active space is named (5241). In the O-loss dissociation, this full valence active space included the $4\sigma^+-9\sigma^+$ and $1\pi-3\pi$ orbits within the $C_{\infty v}$ point group. In the O-loss dissociation calculations these active orbitals were labeled within the C_{2v} (denoted as C_{2v}(a); with the C_2-axis along the O_1-C (O_2-C) bond; see Figure 1) subgroup in the order A_1, B_1, B_2, and A_2 and the full valence active space is named (6330). In all the CASPT2 calculations, the weight values of the CASSCF reference functions in the first-order wave functions were larger than 0.85.

On the basis of the CASPT2 energy calculations for the electronic states of the CO_2^+ ion at the experimental geometry[30] of the ground-state CO_2 molecule, we obtained the CASPT2 vertical relative energies (denoted by T_v') of the excited states to the ground state (X $^2\Pi_g$) of the CO_2^+ ion. We performed the CASPT2 geometry optimization calculations for the electronic states (the CASSCF geometry optimization and frequency analysis calculations were performed), and we obtained the CASPT2 equilibrium geometries and CASPT2 adiabatic relative energies (denoted as T_0, corrected with the CASSCF zero-point energies) of the excited states to the ground state of the CO_2^+ ion.

We calculated O-loss dissociation PECs for the X $^2\Pi_g$ (1 $^2\Pi$), A $^2\Pi_u$ (2 $^2\Pi$), B $^2\Sigma_u^+$ (1 $^2\Sigma^+$), C $^2\Sigma_g^+$ (2 $^2\Sigma^+$), 1 $^4\Sigma_g^-$ (1 $^4\Sigma^-$), and 1 $^4\Pi_u$ (1 $^4\Pi$) states of the CO_2^+ ion at the CASPT2 level. At a set of fixed $R(C-O_1)$ (see Figure 1) values ranging from the $R(C-O_1)$ values in the CASPT2 optimized geometries of the respective states (from 1.20 and 1.40 Å for the repulsive 1 $^4\Pi$ and 1 $^4\Sigma^-$ states, respectively) to 5.0 Å, the CASPT2 partial geometry optimization calculations were performed. The CASPT2 O-loss dissociation PECs for the different states of the CO_2^+ ion were drawn on the basis of the CASPT2 energies at the different sets of partially optimized geometries. The CO_2^+ systems in the different states at the $R(C-O_1)$ value of 5.0 Å are called asymptote products for the respective states. For studying nonadiabatic dissociation processes we performed the CASSCF MECP calculations (in the $C_{\infty v}$, C_s, and C_{2v} symmetries) for the state/state pairs which may be involved in predissociation mechanisms of the C $^2\Sigma_g^+$ state, and then we calculated the CASPT2 energies and CASSCF spin−orbital coupling values at the located MECPs. In the present article, the evaluated energy differences, except the CASPT2 T_0's, were not corrected for zero-point energies.

3. Results and Discussion

3.1. Electronic States of the CO_2^+ Ion. In Table 1 are the CAS results for the X $^2\Pi_g$, A $^2\Pi_u$, B $^2\Sigma_u^+$, C $^2\Sigma_g^+$, 1 $^4\Pi_u$, and 1 $^4\Sigma_g^-$ states of the CO_2^+ ion calculated at the experimental geometry ($R(C-O)$ = 1.162 Å)[30] of the ground-state CO_2 molecule, including the CASPT2 T_v' values and the important configurations in the CASSCF wave functions. The data in the last column in Table 1 show that all the six states have the dominant configurations in their CASSCF wave functions. These dominant configurations indicate that the X $^2\Pi_g$, A $^2\Pi_u$, B $^2\Sigma_u^+$, and C $^2\Sigma_g^+$ states are the primary ionization states and the 1 $^4\Pi_u$ and 1 $^4\Sigma_g^-$ states are the shakeup ionization states.

The CASPT2 T_v' values of 3.73, 4.14, and 5.33 eV for the A $^2\Pi_u$, B $^2\Sigma_u^+$, and C $^2\Sigma_g^+$ states are 0.09, 0.16, and 0.28 eV smaller than the experimental T_v' values from ref 8 (evaluated using the experimental vertical ionization energy values), respectively. The previously reported MRCI T_v' values[31] seem

TABLE 1: CAS Results for the Six Electronic States[a] of the CO_2^+ Ion Calculated at the Experimental Geometry[b] of the Ground-State CO_2 Molecule, Including the CASPT2 Vertical Relative Energies (T_v', in eV) and Important Configurations in the CASSCF Wavefunctions

	T_v'					
state	CASPT2	MRCI[c] (ref 31)	ext[d] (ref 8)	ext[d] (refs 5−7)	important configurations[e]	
X $^2\Pi_g$	0.0	0.0	0.0	0.0	$(1\pi_g)^{-1}$	(0.938)
A $^2\Pi_u$	3.73	3.86	3.82	3.54	$(1\pi_u)^{-1}$	(0.887)
B $^2\Sigma_u^+$	4.14	4.34	4.30	4.30	$(3\sigma_u)^{-1}$	(0.919)
C $^2\Sigma_g^+$	5.33	5.60	5.61	5.61	$(4\sigma_g)^{-1}$	(0.904)
1 $^4\Pi_u$	8.26	8.49			$(1\pi_g)^{-2}(2\pi_u)^{+1}$	(0.930)
1 $^4\Sigma_g^-$	10.22	11.34			$(1\pi_g)^{-}(5\sigma_g)^{+1}$	(0.919)

[a] Including the four lowest-lying primary ionization states (X, A, B, and C) and the two quartet states which are involved in predissociation of the C state. [b] Reference 30 (R(C−O) = 1.162 Å). [c] Calculated at a geometry with R(C−O) = 1.175 Å. [d] Evaluated using the reported experimental vertical ionization energies. [e] The ground-state CO_2 molecule has electronic configuration of ...$(4\sigma_g)^2$ $(3\sigma_u)^2$ $(1\pi_u)^4$ $(1\pi_g)^4$ $(2\pi_u)^0$ $(5\sigma_g)^0$.

TABLE 2: CASPT2 Adiabatic Relative Energies (T_0, in eV) and CASPT2 Optimized Geometries for the Six (Seven) States[a] of the CO_2^+ Ion (Bond Lengths in Å and Bond Angles in Degrees; for Notations, see Figure 1)

		T_0		geometry		
state		CASPT2	ext[b]	R(C−O_1)	R(C−O_2)	∠OCO
X $^2\Pi_g$		0.0	0.0	1.173(1.177)[c]	1.173 (1.177)	180.0 (180.0)
A $^2\Pi_u$		3.49	3.53	1.225 (1.227)	1.225 (1.227)	180.0 (180.0)
B $^2\Sigma_u^+$		4.15	4.29	1.172 (1.180)	1.172 (1.180)	180.0 (180.0)
C $^2\Sigma_g^+$		5.45	5.60	1.149 (1.155)	1.149 (1.155)	180.0 (180.0)
1 $^4\Pi_u$	1 $^4A_1$	7.74		1.284	1.284	111.2
	1 $^4B_1$	3.97		1.264	1.264	108.7
1 $^4\Sigma_g^-$	1 $^4\Sigma^-$	3.80		2.021	1.117	180.0

[a] Including the four lowest-lying primary ionization states (X, A, B, and C) and the two quartet states which are involved in predissociation of the C state. The 1 $^4\Pi_u$ state splits into the 1 $^4A_1$ and 1 $^4B_1$ states. [b] Evaluated using the experimental adiabatic ionization energy data reported in ref 32. [c] Values in parentheses are the experimental geometric data reported in ref 32.

to be in better agreement with the experimental values.[8] We note that the MRCI calculations[31] were performed at a geometry with the R(C−O) value of 1.175 Å. The CASPT2 T_v' values for the 1 $^4\Pi_u$ and 1 $^4\Sigma_g^-$ states are 8.26 and 10.22 eV, respectively, and experimental T_v' values are not available for these shakeup ionization states.

In Table 2 are the CASPT2 T_0 values and optimized geometries for the X $^2\Pi_g$, A $^2\Pi_u$, B $^2\Sigma_u^+$, C $^2\Sigma_g^+$, 1 $^4\Pi_u$, and 1 $^4\Sigma_g^-$ states of the CO_2^+ ion. Our CASPT2 geometry optimization calculations indicate that (i) the X $^2\Pi_g$, A $^2\Pi_u$, B $^2\Sigma_u^+$, and C $^2\Sigma_g^+$ states have the $D_{\infty h}$ equilibrium geometries; (ii) the Renner−Teller splitting in 1 $^4\Pi_u$ lead to two C_{2v} states, 1 $^4A_1$ and 1 $^4B_1$, and the OCO angles in the two C_{2v} equilibrium geometries are around 110° (see Table 2); and (iii) the 1 $^4\Sigma_g^-$ (1 $^4\Sigma^-$) state has a $C_{\infty v}$ geometry with one long C−O bond of 2.021 Å and is not a purely repulsive state. These conclusions were confirmed by the CASSCF frequency analysis calculations at the CASSCF optimized geometries (the explicit frequency values predicted by the CASSCF calculations will not be reported since they are not so accurate). On the basis of their calculations, the authors of ref 5 reported a C $^2\Sigma_g^+$ geometry identical to our CASPT2 geometry and mentioned the long C−O bond in the 1 $^4\Sigma^-$(1 $^4\Sigma_g^-$) geometry.

The CASPT2 T_0 values of 3.49, 4.15, and 5.45 eV for the A $^2\Pi_u$, B $^2\Sigma_u^+$, and C $^2\Sigma_g^+$ states are 0.04, 0.14, and 0.15 eV smaller than the experimental T_0 values[32] (evaluated using the experimental adiabatic ionization energy values), respectively. The C−O bond length values in the CASPT2 geometries of the X $^2\Pi_g$, A $^2\Pi_u$, B $^2\Sigma_u^+$, and C $^2\Sigma_g^+$ states are 0.004, 0.002, 0.008, and 0.006 Å smaller than the experimental bond length values,[32] respectively. The CASPT2 geometry optimization calculations for the X, A, B, and C states produced accurate results (T_0's and geometries). The large T_0 difference between the 1 $^4A_1$ and 1 $^4B_1$ states indicates a large splitting.

TABLE 3: Four Lowest O-Loss Dissociation Limits (Dissociation Product Groups) of the CO_2^+ Ion, Together with the CASPT2 and Experimental Sum Energy Values (ΔE, in eV) for the Product Groups Relative to CO_2^+ (X $^2\Pi_g$)

	ΔE			
product groups	CASPT2	expt[b]	expt[c]	states of the CO_2^+ ion[a]
1 O^+ (^4S_u) + CO (X $^1\Sigma^+$)	5.29	5.30	5.27	$^4\Sigma^-$ (1 $^4\Sigma_g^-$)
2 O (^3P_g) + CO^+ (X $^2\Sigma^+$)	5.84	5.69	5.67	$^{2,4}\Sigma^-$, $^{2,4}\Pi$ (X $^2\Pi_g$, 1 $^4\Pi_u$)
3 O (^1D_g) + CO^+ (X $^2\Sigma^+$)	7.81	7.66		$^2\Pi$, $^2\Sigma^+$, $^2\Delta$ (A $^2\Pi_u$, B $^2\Sigma_u^+$)
4 O (^3P_g) + CO^+ (A $^2\Pi$)	8.39	8.20		$^{2,4}\Sigma^+$, $^{2,4}\Sigma^-$, $^{2,4}\Pi$, $^{2,4}\Delta$ (C $^2\Sigma_g^+$)

[a] In parentheses are the CO_2^+ states calculated in the present work. [b] From ref 33. [c] From ref 5.

3.2. O-Loss Dissociation Potential Energy Curves. For evaluating the CASPT2 sum energies for the O-loss dissociation product groups, we performed the CASPT2 geometry optimization calculations for CO (X $^1\Sigma^+$), CO^+ (X $^2\Sigma^+$), and CO^+ (A $^2\Pi$) (the optimized bond length values being 1.128, 1.116, and 1.241 Å, respectively) and the CASPT2 energy calculations for O^+ (^4S_u), O (^3P_g), and O (^1D_g). In Table 3 are the CASPT2 sum energies of the five lowest O-loss dissociation product groups relative to the X $^2\Pi_g$ reactant ("sum energy of the product group relative to the X $^2\Pi_g$ reactant" will be abbreviated to "sum energy of the product group" in the rest of the article), together with the experimental sum energies of the five product groups.[5,33] The CASPT2 sum energies of the O^+ (^4S_u) + CO (X $^1\Sigma^+$), O (^3P_g) + CO^+ (X $^2\Sigma^+$), O (^1D_g) + CO^+ (X $^2\Sigma^+$), and O (^3P_g) + CO^+ (A $^2\Pi$) product groups are 5.29, 5.84, 7.81, and 8.39 eV, respectively, which are in good agreement with the respective experimental sum energies[5,33] (the deviations being smaller than 0.20 eV). The CO_2^+ states correlating with these product groups are listed in the last column of Table 3.

The CASPT2 O-loss dissociation PECs of the X $^2\Pi_g$ (1 $^2\Pi$), A $^2\Pi_u$ (2 $^2\Pi$), B $^2\Sigma_u^+$ (1 $^2\Sigma^+$), C $^2\Sigma_g^+$ (2 $^2\Sigma^+$), 1 $^4\Sigma_g^-$ (1 $^4\Sigma^-$), and 1 $^4\Pi_u$ (1 $^4\Pi$) states of the CO_2^+ ion are drawn in Figure 2. The CASPT2 energies of the reactants and the asymptote products relative to X$^2\Pi_g$ are given in Figure 2 ("CASPT2 energy of the reactants (the asymptote products) relative to X $^2\Pi_g$" will be abbreviated to "CASPT2 energy of the reactants (the asymptote products)" in the rest part of the article).

The CASPT2 energy value (5.42 eV) of the 1 $^4\Sigma_g^-$ asymptote product is close to the CASPT2 sum energy value (5.29 eV) of the O^+ (^4S_u) + CO (X $^1\Sigma^+$) product group. In the 1 $^4\Sigma_g^-$ asymptote product, the Mulliken charge value at the O_1 center is +1.004 e and the C−O_2 bond length value is 1.125 Å (close to the CASPT2 bond length value of 1.128 Å in CO (X $^1\Sigma^+$)). These facts indicate that the 1 $^4\Sigma_g^-$ state correlates with O^+ (^4S_u) + CO (X $^1\Sigma^+$) (the first dissociation limit). The CASPT2 energy values of the X $^2\Pi_g$ and 1 $^4\Pi_u$ asymptote products (5.86 and 5.81 eV, respectively) are very close to the CASPT2 sum energy value (5.84 eV) of the O (^3P_g) + CO^+ (X $^2\Sigma^+$) product group. In the two asymptote products the Mulliken charge values at the O_1 center are around 0.000 e and the C−O_2 bond length values are both 1.116 Å (equal to the CASPT2

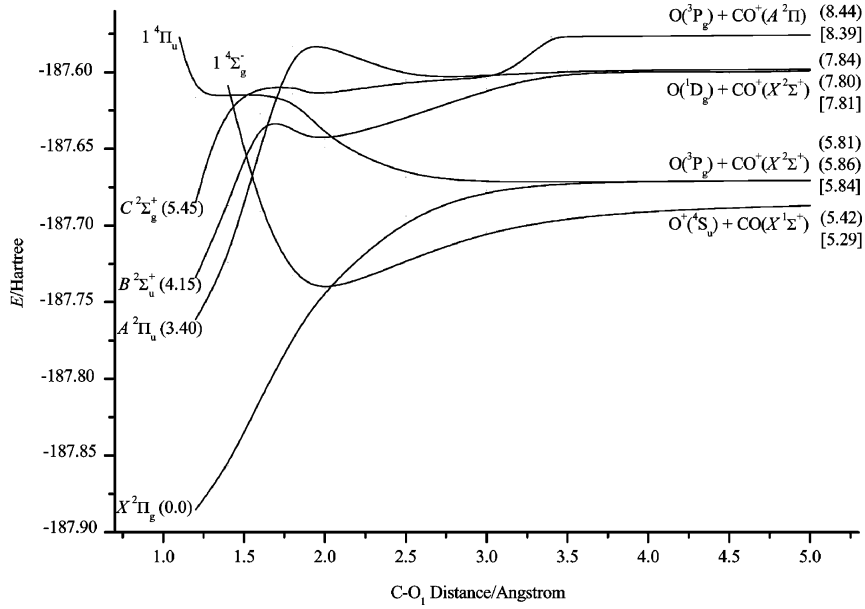

Figure 2. CASPT2 potential energy curves for O-loss dissociation from the X $^2\Pi_g$, A $^2\Pi_u$, B $^2\Sigma_u^+$, C $^2\Sigma_g^+$, 1 $^4\Sigma_g^-$, and 1 $^4\Pi_u$ states of the CO_2^+ ion. The values in parentheses are the CASPT2 energies (in eV) of the reactants and asymptote products relative to the X $^2\Pi_g$ reactant and the values in square brackets are the CASPT2 sum energies (in eV) of the product groups relative to the X $^2\Pi_g$ reactant (the experimental sum energies of the product groups are given in Table 3).

bond length value in CO^+ (X $^2\Sigma^+$)). These facts indicate that the X $^2\Pi_g$ and 1 $^4\Pi_u$ states correlate with O (^3P_g) + CO^+ (X $^2\Sigma^+$) (the second dissociation limit). The CASPT2 energy values of the A $^2\Pi_u$ and B $^2\Sigma_u^+$ asymptote products (7.80 and 7.84 eV, respectively) are very close to the CASPT2 sum energy value (7.81 eV) of the O (^1D_g) + CO^+ (X $^2\Sigma^+$) product group. In the two asymptote products the Mulliken charge values at the O_1 center are around 0.000 *e* and the C−O_2 bond length values are both 1.116 Å (equal to the CASPT2 bond length value in CO^+ (X $^2\Sigma^+$)). These facts indicate that the A $^2\Pi_u$ and B $^2\Sigma_u^+$ states correlate with O (^1D_g) + CO^+ (X $^2\Sigma^+$) (the third dissociation limit). The CASPT2 energy value (8.44 eV) of the C $^2\Sigma_g^+$ asymptote product is very close to the CASPT2 sum energy value (8.39 eV) of the O (^3P_g) + CO^+ (A $^2\Pi$) product group. In the C $^2\Sigma_g^+$ asymptote product the Mulliken charge value at the O_1 center is −0.015 *e* (close to zero) and the C−O_2 bond length value is 1.242 Å (close to the CASPT2 bond length value of 1.241 Å in CO^+ (A $^2\Pi$)). These facts indicate that the C $^2\Sigma_g^+$ state correlates with O (^3P_g) + CO^+ (A $^2\Pi$) (the fourth dissociation limit). As shown in Table 3, each of the third and fourth dissociation limits correlates with one $^2\Sigma^+$ state of CO_2^+. It is rational that the B$^2\Sigma_u^+$ state is the $^2\Sigma^+$ state correlating to the third limit while the C$^2\Sigma_g^+$ state is the $^2\Sigma^+$ state correlating to the fourth limit.[19,21]

As shown in Figure 2, there are transition states along the A $^2\Pi_u$ and B $^2\Sigma_u^+$ PECs and intermediates (shallow minima) along the A $^2\Pi_u$, B $^2\Sigma_u^+$, C $^2\Sigma_g^+$, and 1 $^4\Sigma_g^-$ PECs. The 1 $^4\Pi_u$ PEC is essentially repulsive. In Figure 2 the 1 $^4\Sigma_g^-$ PEC crosses the other five PECs and the 1 $^4\Pi_u$ PEC crosses the 1 $^4\Sigma_g^-$, C $^2\Sigma_g^+$, A $^2\Pi_u$, and B $^2\Sigma_u^+$ PECs.

The CASSCF PECs for the X $^2\Pi_g$, A $^2\Pi_u$, B $^2\Sigma_u^+$, 1 $^4\Sigma_g^-$ (a $^4\Sigma_g^-$), and 1 $^4\Pi_u$ (b $^4\Pi_u$) states of the CO_2^+ ion given in Figure 8 of ref 5 have features similar to those of the CASPT2 PECs for the respective states, but the CASSCF PEC for C $^2\Sigma_g^+$ does not have features similar to those of the CASPT2 PEC. As stated by the authors of ref 5, the energies of the dissociation limits and electronic states were shifted to known experimental values in that figure, and those CASSCF PECs did not well converge to the dissociation product groups. The PECs of good quality should be drawn on the basis of partially geometry optimization calculations using an accurate and size-consistent quantum-chemical method (for example, CASPT2 method plus the full valence active spaces for all the species involved).

3.3. Predissociation of the C $^2\Sigma_g^+$ State. ***3.3.1. MECP Calculations.*** In Table 4 are the geometries of the CASSCF MECPs for the C $^2\Sigma_g^+$/1 $^4\Sigma_g^-$, C $^2\Sigma_g^+$/1 $^4\Pi_u$, 1 $^4\Pi_u$/1 $^4\Sigma_g^-$, 1 $^4\Sigma_g^-$/X $^2\Pi_g$, and A $^2\Pi_u$/1 $^4\Sigma_g^-$ state/state pairs, together with the CASSCF spin−orbit coupling values and CASPT2 state/state energies (relative to X $^2\Pi_g$) calculated at the CASSCF MECP geometries. At each of the located MECPs, the CASSCF energy difference between the two states in the pair is smaller than 0.05 eV and the CASPT2 energy difference is smaller than 0.45 eV (we will use the average of the CASPT2 energies in discussion).

MECP for a state/state pair is a special crossing point (a geometry) between the two potential energy surfaces (PES's). It is not the crossing point between the two PECs (if the two PECs cross in the PEC figure) and may not be along either of the PECs. A MECP may have a geometry of the $C_{\infty v}$, C_s, or C_{2v}(b) symmetry. We performed the MECP calculations for the selected state/state pairs in the $C_{\infty v}$, C_s, and C_{2v}(b) symmetries (the notations of the states in pairs will be changed thereby).

The CASSCF MECP calculations for the C $^2\Sigma_g^+$/1 $^4\Sigma_g^-$, 1 $^4\Pi_u$/1 $^4\Sigma_g^-$, 1 $^4\Sigma_g^-$/X $^2\Pi_g$, and A $^2\Pi_u$/1 $^4\Sigma_g^-$ state pairs were performed in the $C_{\infty v}$ symmetry and the state/state notations become 2 $^2\Sigma^+$/1 $^4\Sigma^-$, 1 $^4\Pi$/1 $^4\Sigma^-$, 1 $^4\Sigma^-$/1 $^2\Pi$, and 2 $^2\Pi$/1 $^4\Sigma^-$, respectively (see the second column of Table 4). In the MECP calculations within the C_{2v}(a) subgroup of $C_{\infty v}$, the B_1 and B_2 components of Π led to the same MECP results (geometries, energies, and spin−orbit couplings). As shown in Table 4, the MECP geometries for the C $^2\Sigma_g^+$/1 $^4\Sigma_g^-$, 1 $^4\Pi_u$/1 $^4\Sigma_g^-$, 1 $^4\Sigma_g^-$/X $^2\Pi_g$, and A $^2\Pi_u$/1 $^4\Sigma_g^-$ state pairs have the $C_{\infty v}$ symmetry, and the calculated spin−orbit couplings at the four MECPs are 6.0, 33.7, 169.6, and 187.3 cm^{-1}, respectively. The small value (6.0 cm^{-1}) at the C $^2\Sigma_g^+$/1 $^4\Sigma_g^-$ MECP is in line with the selection rule for predissociation.[30]

The CASSCF MECP calculations for the C $^2\Sigma_g^+$/1 $^4\Pi_u$ state pair were first performed in the $C_{\infty v}$ symmetry, and the state/

TABLE 4: Locations (Geometries) of Minimum Energy Crossing Points (MECPs) for Selected State/State Pairs (Possibly Involved in Predissociation Mechanisms of the C $^2\Sigma_g^+$ State) Predicted by the CASSCF Calculations, Together with the CASSCF Spin−Orbit Coupling Values (in cm^{-1}) and CASPT2 State/State Energies ($\Delta E/\Delta E$ in eV, Relative to X $^2\Pi_g$) at the CASSCF MECPs (Bond Lengths in Å and Bond Angles in Degrees)[a]

MECP (state/state)		MECP geometry			spin−orbit coupling	CASPT2 $\Delta E/\Delta E$
		R(C−O$_1$)	R(C−O$_2$)	∠OCO		
C $^2\Sigma_g^+$/1 $^4\Sigma_g^-$	2 $^2\Sigma^+$/1 $^4\Sigma^-$	1.386	1.159	180.0	6.0	7.33/7.73
C $^2\Sigma_g^+$/1 $^4\Pi_u$	2 $^2\Sigma^+$/1 $^4\Pi$	1.300	1.300	180.0	0.0	7.13/7.15
	4 ^{2}A′/1 ^{4}A′ (1 ^{4}A$_1$)	1.491	1.491	87.0	0.0	8.95/8.81
	4 ^{2}A′/1 ^{4}A″ (1 ^{4}B$_1$)	1.489	1.489	87.0	77.7	8.95/8.87
1 $^4\Pi_u$/1 $^4\Sigma_g^-$	1 $^4\Pi$/1 $^4\Sigma^-$	1.405	1.256	180.0	33.7	7.40/7.77
1 $^4\Sigma_g^-$/X $^2\Pi_g$	1 $^4\Sigma^-$/1 $^2\Pi$	2.041	1.122	180.0	169.6	3.84/4.10
A $^2\Pi_u$ /1 $^4\Sigma_g^-$	2 $^2\Pi$/1 $^4\Sigma^-$	1.530	1.204	180.0	187.3	5.94/6.23

[a] See text for the materials presented in the second column.

state notation becomes 2 $^2\Sigma^+$/1 $^4\Pi$. In the MECP calculations within the C_{2v}(a) subgroup of $C_{\infty v}$, the 1 ^{4}B$_1$ and 1 ^{4}B$_2$ components of 1 $^4\Pi$ led to the same MECP results: a $D_{\infty h}$ MECP geometry and a spin−orbit coupling value of zero. Then we performed the MECP calculations in the C_s symmetry, and the C $^2\Sigma_g^+$/1 $^4\Pi_u$ state pair becomes the 4 ^{2}A′/1 ^{4}A′ and 4 ^{2}A′/1 ^{4}A″ state pairs. The MECP calculations for the 4 ^{2}A′/1 ^{4}A′ state pair led to a C_{2v}(b) MECP geometry (R(C−O) = 1.491 Å, ∠OCO = 87.0°), and the 1 ^{4}A′ component of 1 $^4\Pi_u$ (in C_s) becomes the 1 ^{4}A$_1$ component of 1 $^4\Pi_u$ (in C_{2v}(b)). The MECP calculations for the 4 ^{2}A′/1 ^{4}A″ state pair led to another C_{2v}(b) MECP geometry (R(C−O) = 1.489 Å, ∠OCO = 87.0°), and the 1 ^{4}A″ component of 1 $^4\Pi_u$ (in C_s) becomes the 1 ^{4}B$_1$ component of 1 $^4\Pi_u$ (in C_{2v}(b)). The C_{2v}(b) geometries (and energies) at the 4 ^{2}A′/1 ^{4}A′ (1 ^{4}A$_1$) and 4 ^{2}A′/1 ^{4}A″ (1 ^{4}B$_1$) MECPs are almost identical. The CASSCF spin−orbit coupling value at the 4 ^{2}A′/1 ^{4}A′ (1 ^{4}A$_1$) MECP is zero, while the value at the 4 ^{2}A′/1 ^{2}A″ (1 ^{4}B$_1$) MECP is 77.7 cm^{-1}. Since the spin−orbit coupling values are different, we should explicitly write two MECPs for the C $^2\Sigma_g^+$/1 $^4\Pi_u$ state pair: C $^2\Sigma_g^+$/1 $^4\Pi_u$ (1 ^{4}A$_1$) and C $^2\Sigma_g^+$/1 $^4\Pi_u$ (1 ^{4}B$_1$) MECPs. The ^{4}B$_1$ state was mentioned in refs 5, 20, and 21, and the C $^2\Sigma_g^+$/1 $^4\Pi_u$ (1 ^{4}B$_1$) MECP with a large spin−orbit coupling value of 77.7 cm^{-1} is important for the predissociation mechanism of the C $^2\Sigma_g^+$ state (see below). The CASPT2 energy (relative to X$^2\Pi_g$) of the C $^2\Sigma_g^+$/1 $^4\Pi_u$ (1 ^{4}B$_1$) [4 ^{2}A′/1 ^{4}A″ (1 ^{4}B$_1$)] MECP is around 8.9 eV, which is an important datum for the following discussion on predissociation mechanisms of the C $^2\Sigma_g^+$ state.

3.3.2. Discussion on the Predissociation Mechanism Suggested in Ref 21. The predissociation mechanism of the C $^2\Sigma_g^+$ state suggested by Praet et al.[21] consists of processes I, II, and III (see Introduction). In our calculations we have found the C $^2\Sigma_g^+$/1 $^4\Pi_u$ (1 ^{4}B$_1$) MECP, 1 $^4\Pi_u$/1 $^4\Sigma_g^-$ MECP (conical intersection), and 1 $^4\Sigma_g^-$/X $^2\Pi_g$ MECP for processes I, II, and III, respectively, and the calculated spin−orbit coupling values at these MECPs are large. Therefore, our calculations support the predissociation mechanism of the C $^2\Sigma_g^+$ state suggested by Praet et al.[21] We can rewrite processes I, II, and III by adding the calculated MECPs and relevant data along the processes: (I) CO_2^+ (C $^2\Sigma_g^+$) (5.45 eV) → C $^2\Sigma_g^+$/1 $^4\Pi_u$ (1 ^{4}B$_1$) MECP (≈8.9 eV, 77.7 cm^{-1}) → CO_2^+ (1 $^4\Pi_u$) → O (^{3}P$_g$) + CO^+ (X $^2\Sigma^+$) (5.81 eV, the second dissociation limit); (II) CO_2^+ (1 $^4\Pi_u$) → 1 $^4\Pi_u$/1 $^4\Sigma_g^-$ MECP (conical, ≈7.6 eV, 33.7 cm^{-1}) → CO_2^+(1 $^4\Sigma_g^-$) (3.80 eV) → O^+ (^{4}S$_u$) + CO (X $^1\Sigma^+$) (5.42 eV, the first dissociation limit); and (III) CO_2^+ (1 $^4\Sigma_g^-$) (3.80 eV) → 1 $^4\Sigma_g^-$/X $^2\Pi_g$ MECP (≈3.9 eV, 169.6 cm^{-1}) → CO_2^+ (X $^2\Pi_g$) → O (^{3}P$_g$) + CO^+ (X $^2\Sigma^+$) (5.86 eV, the second dissociation limit). In parentheses, the quantities in eV are the CASPT2 relative energy values to CO_2^+ (X $^2\Pi_g$) and the quantities in cm^{-1} are the CASSCF spin−orbit coupling values at the MECPs. The maximum CASPT2 relative energy value is 8.9 eV at the C $^2\Sigma_g^+$/1 $^4\Pi_u$ (1 ^{4}B$_1$) MECP, indicating that for following this mechanism the ionic system needs an energy of 8.9 eV from CO_2^+ (X $^2\Pi_g$). Since the C $^2\Sigma_g^+$/1 $^4\Pi_u$ (1 ^{4}A$_1$) MECP has a spin−orbit coupling value of zero, it does not appear in the rewritten processes.

Praet et al.[21] (and Yang et al.[20]) also considered an extra process (1 $^4\Pi_u$ → X $^2\Pi_g$) following process I. In Figure 2 the 1 $^4\Pi_u$ and X $^2\Pi_g$ PECs do not cross. However, we found the MECP for the 1 $^4\Pi_u$ (1 ^{4}B$_1$)/X $^2\Pi_g$ pair in the C_{2v}(b) symmetry in the CASSCF calculations and the calculated spin−orbit coupling values were larger than 35 cm^{-1} (the results are not given in Table 4).

3.3.3. Discussion on the Predissociation Mechanisms in the Two Previous Experiments. In the [1 + 1] photodissociation experiments of Yang et al.,[20] the two-photon energy of 7.06−9.72 eV was comparable with the energy of 8.9 eV needed in the predissociation mechanism for the C $^2\Sigma_g^+$ state suggested by Praet et al.[21] Therefore, in the experiments of Yang et al.[20] the C $^2\Sigma_g^+$ state of CO_2^+ could predissociate through the mechanism suggested by Praet et al.[21]

In the VUV-PFI-PE experiments of Liu et al.,[5] the highest energy of the system is 0.41 eV (relative to C $^2\Sigma_g^+$). When the experimental T_0 energy of 5.60 eV[32] for C $^2\Sigma_g^+$ is added, the highest energy value becomes 6.01 eV (relative to X $^2\Pi_g$), which is smaller than the energy value of 8.9 eV needed in the predissociation mechanism for the C $^2\Sigma_g^+$ state suggested by Praet et al.[21] Another predissociation mechanism (process IV, see Introduction) of the C $^2\Sigma_g^+$ state via A $^2\Pi_u$ was proposed by Liu et al.[5] We can rewrite process IV by adding the calculated MECP and relevant data: (IV) CO_2^+ (C $^2\Sigma_g^+$) (5.45 eV) → CO_2^+ (A $^2\Pi_u$) (3.49 eV, $f = 0.2424 \times 10^{-3}$) → A $^2\Pi_u$/1 $^4\Sigma_g^-$ MECP (≈6.1 eV, 187.3 cm^{-1}) → CO_2^+ (1 $^4\Sigma_g^-$) (3.80 eV) → O^+ (^{4}S$_u$) + CO (X $^1\Sigma^+$) (5.42 eV, the first dissociation limit). The results for the A $^2\Pi_u$/1 $^4\Sigma_g^-$ MECP were already given in Table 4. We used the CAS state interaction (CASSI) method[34,35] to compute the oscillator strength f value, using the energy difference corrected by the CASPT2 calculations, for the A $^2\Pi_u$ ← C $^2\Sigma_g^+$ transition, and the calculated f value of 0.2424×10^{-3} is not small. The maximum CASPT2 relative energy value in process IV is 6.1 eV (at the A $^2\Pi_u$/1 $^4\Sigma_g^-$ MECP), which is close to the highest energy value of 6.01 eV. Therefore, the C $^2\Sigma_g^+$ state of CO_2^+, in the VUV-PFI-PE experiments of Liu et al.,[5] predissociated not through the mechanism suggested by Praet et al.,[21] but through process IV (via A $^2\Pi_u$). We would mention that process IV may also be followed by process III, which starts from the fourth species in process IV, leading to O (^{3}P$_g$) + CO^+ (X $^2\Sigma^+$) (the second dissociation limit).

4. Conclusions

In the present study we calculated the X $^2\Pi_g$, A $^2\Pi_u$, B $^2\Sigma_u^+$, C $^2\Sigma_g^+$, 1 $^4\Sigma_g^-$, and 1 $^4\Pi_u$ states of the CO_2^+ ion using the CAS methods,[22−24] and the main purpose was to study the predissociation mechanism of the C $^2\Sigma_g^+$ state. The CASPT2 calculations indicate that the Renner−Teller splitting in 1 $^4\Pi_u$ leads to two C_{2v} states (1 $^4A_1$ and 1 $^4B_1$) and the OCO bond angles in the two C_{2v} equilibrium geometries are around 110° and that the 1 $^4\Sigma_g^-$ (1 $^4\Sigma^-$) state is not a purely repulsive state and has a $C_{\infty v}$ geometry with one long C−O bond of 2.021 Å. The CASPT2 T_0 values and geometries for the X $^2\Pi_g$, A $^2\Pi_u$, B $^2\Sigma_u^+$, and C $^2\Sigma_g^+$ states are in good agreement with experiment.[32]

The CASPT2 O-loss dissociation PECs were calculated for the six states on the basis of the partial geometry optimization calculations. On the basis of the calculated energies and properties for the asymptote products (at R(C−O$_1$) = 5.0 Å), we conclude that (i) the 1 $^4\Sigma_g^-$ state correlates with O^+ (^4S_u) + CO (X $^1\Sigma^+$) (the first limit); (ii) the X $^2\Pi_g$ and 1 $^4\Pi_u$ states correlate with O (^3P_g) + CO^+ (X $^2\Sigma^+$) (the second limit); (iii) the A $^2\Pi_u$ and B $^2\Sigma_u^+$ states correlate with O (^1D_g) + CO^+ (X $^2\Sigma^+$) (the third limit); and (iv) the C $^2\Sigma_g^+$ state correlates with O (^3P_g) + CO^+ (A $^2\Pi$) (the fourth limit). The CASPT2 energy (see section 3.2) values of the asymptote products are very close to the CASPT2 sum energy (see section 3.2) values of the product groups, respectively, indicating that the calculation approach (CASPT2 plus full valence active spaces) is size-consistent. The CASPT2 sum energy values of the product groups are very close to the experimental sum energy values,[5,33] respectively, indicating the calculation approach is accurate.

We performed the CASSCF MECP calculations (in the $C_{\infty v}$, C_s, and C_{2v} symmetries) for the C $^2\Sigma_g^+$ /1 $^4\Sigma_g^-$, C $^2\Sigma_g^+$ /1 $^4\Pi_u$, 1 $^4\Pi_u$/1 $^4\Sigma_g^-$, 1 $^4\Sigma_g^-$/X $^2\Pi_g$, and A $^2\Pi_u$/1 $^4\Sigma_g^-$ state pairs and calculated the CASSCF spin−orbit coupling values and CASPT2 energies at these MECPs. One should explicitly write two MECPs for the C $^2\Sigma_g^+$/1 $^4\Pi_u$ state pair: C $^2\Sigma_g^+$/1 $^4\Pi_u$ (1 $^4A_1$) MECP and C $^2\Sigma_g^+$/1 $^4\Pi_u$ (1 $^4B_1$) MECP, since the spin−orbit couplings at the two MECPs are different (zero and 77.7 cm^{-1}, respectively). The C $^2\Sigma_g^+$/1 $^4\Pi_u$ (1 $^4B_1$) MECP with a large spin−orbit coupling value is important.

On the basis of our calculation results (the PECs, the MECPs, and the spin−orbit coupling and f values), we discussed the predissociation mechanisms of the C $^2\Sigma_g^+$ state suggested in refs 5, 20, and 21. The predissociation mechanism of the C $^2\Sigma_g^+$ state suggested by Praet et al.[21] consists of processes I, II, and III. In our calculations we have found the C $^2\Sigma_g^+$/1 $^4\Pi_u$ (1 $^4B_1$) MECP, 1 $^4\Pi_u$/1 $^4\Sigma_g^-$ MECP (conical intersection), and 1 $^4\Sigma_g^-$/X $^2\Pi_g$ MECP, which are critical for processes I, II, and III, respectively, and the calculated spin−orbit couplings at these MECPs are large (not very small or zero). Therefore, our CAS calculations support the predissociation mechanism of the C $^2\Sigma_g^+$ state suggested by Praet et al.[21] However, our CASPT2 calculations indicate that for following this mechanism the ionic system needs energy of 8.9 eV from CO_2^+ (X $^2\Pi_g$). Since the two-photon energy of 7.06−9.72 eV in the [1 + 1] photodissociation experiments of Yang et al.[20] was comparable with the energy of 8.9 eV, the C $^2\Sigma_g^+$ state of CO_2^+ in their experiments could predissociate through the mechanism suggested by Praet et al.[21]

In the experiments of Liu et al.,[5] the highest energy of the system (relative to X $^2\Pi_g$) was 6.01 eV, which is significantly smaller than 8.9 eV. The C $^2\Sigma_g^+$ state of CO_2^+ in their experiments predissociated not through the mechanism suggested by Praet et al.,[21] but through another predissociation mechanism via A $^2\Pi_u$ (process IV) proposed by Liu et al.[5] Our calculations indicate that process IV is feasible.

Acknowledgment. We appreciate the financial support of this work that was provided by National Natural Science Foundation of China through Contract No. 20773161.

References and Notes

(1) Dalgarno, A.; Fox, J. L. In *Unimolecular and Bimolecular Ion−Molecule Reaction Dynamics*; Ng, C. Y., Baer, T., Powis, I., Eds.; Wiley: Chichester, U.K., 1994; pp 1.
(2) Baer, T.; Guyon, P. M. *J. Chem. Phys.* **1986**, *85*, 4765.
(3) Gauyacq, D.; Horani, M.; Leach, S.; Rostas, J. *Can. J. Phys.* **1975**, *53*, 2040.
(4) Gauyacq, D.; Larcher, C.; Rostas, J. *Can. J. Phys.* **1979**, *57*, 1634.
(5) Liu, J. B.; Chen, W. W.; Hochlaf, M.; Qian, X. M.; Chang, C.; Ng, C. Y. *J. Chem. Phys.* **2003**, *118*, 149.
(6) Liu, J. B.; Chen, W. W.; Hsu, C. W.; Hochlaf, M.; Evans, M.; Stimson, S.; Ng, C. Y. *J. Chem. Phys.* **2000**, *112*, 10767.
(7) Liu, J. B.; Hochlaf, M.; Ng, C. Y. *J. Chem. Phys.* **2000**, *113*, 7988.
(8) Potts, A. W.; Fattahallah, G. H. *J. Phys. B-At. Mol. Opt. Phys.* **1980**, *13*, 2545.
(9) Wang, L.-S.; Reutt, J. E.; Lee, Y. T.; Shirley, D. A. *J. Electron Spectrosc. Relat. Phenom.* **1988**, *47*, 167.
(10) Baltzer, P.; Chau, F. T.; Eland, J. H. D.; Karlsson, L.; Lundqvist, M.; Rostas, J.; Tam, K. Y.; Veenhuizen, H.; Wannberg, B. *J. Chem. Phys.* **1996**, *104*, 8922.
(11) Merkt, F.; Mackenzie, S. R.; Rednall, R. J.; Softley, T. P. *J. Chem. Phys.* **1993**, *99*, 8430.
(12) Sears, T. J. *Mol. Phys.* **1986**, *59*, 259.
(13) Wannberg, B.; Veenhuizen, H.; Mattsson, L.; Norell, K.-E.; Karlsson, L.; Siegbahn, K. *J. Phys. B-At. Mol. Opt. Phys.* **1984**, *17*, L259.
(14) Bhardwaj, V. R.; Mathur, D.; Vijayalakshmi, K.; Hvelplund, P.; Larsson, M. O.; Safvan, C. P. *Phys. Rev. A* **1998**, *58*, 2834.
(15) González-Magaña, O.; Cabrera-Trujillo, R.; Hinojosa, G. *Phys. Rev. A* **2008**, *78*, 052712.
(16) Mrozowski, S. *Phys. Rev.* **1947**, *72*, 691.
(17) Taylor, D. P.; Johnson, P. M. *J. Chem. Phys.* **1993**, *98*, 1810.
(18) Wu, M.; Taylor, D. P.; Johnson, P. M. *J. Chem. Phys.* **1991**, *94*, 7596.
(19) Wu, M.; Taylor, D. P.; Johnson, P. M. *J. Chem. Phys.* **1991**, *95*, 761.
(20) Yang, M.; Zhang, L.; Zhuang, X.; Lai, L.; Yu, S. *J. Chem. Phys.* **2008**, *128*, 164308.
(21) Praet, M. T.; Lorquet, J. C.; Raseev, G. *J. Chem. Phys.* **1982**, *77*, 4611–4618.
(22) Andersson, K.; Malmqvist, P.; Roos, B. O. In *Modern Electronic Structure Theory, Part 1*; Yarkony, D. R., Ed.; World Scientific: Singapore, 1995, pp 55.
(23) Andersson, K.; Roos, B. O. *Int. J. Quantum Chem.* **1993**, *45*, 591–607.
(24) Roos, B. O. In *Advances in Chemical Physics*; Lawley, K. P., Ed.; Wiley: Chichester, U.K., 2007; pp 399−445.
(25) Karlström, G.; Lindh, R.; Malmqvist, P.-Å.; Roos, B. O.; Ryde, U.; Veryazov, V.; Widmark, P.-O.; Cossi, M.; Schimmelpfennig, B.; Neogrady, P.; Seijo, L. *Comput. Mater. Sci.* **2003**, *28*, 222.
(26) Almlof, J.; Taylor, P. R. *J. Chem. Phys.* **1987**, *86*, 4070–4077.
(27) Pierloot, K.; Dumez, B.; Widmark, P.-O.; Roos, B. O. *Theor. Chem. Acc.: Theory, Comput., Modeling (Theor. Chim. Acta)* **1995**, *90*, 87–114.
(28) Widmark, P.-O.; Malmqvist, P.-Å.; Roos, B. O. *Theor. Chem. Acc.: Theory, Comput., Modeling (Theor. Chim. Acta)* **1990**, *77*, 291–306.
(29) Widmark, P.-O.; Persson, B. J.; Roos, B. O. *Theor. Chem. Acc.: Theory, Comput., Modeling (Theor. Chim. Acta)* **1991**, *79*, 419–432.
(30) Herzberg, G. *Electronic Spectra and Electronic Structure of Polyatomic Molecules*; Van Nostrand: New York, 1966.
(31) Polak, R.; Hochlaf, M.; Levinas, M.; Chambaud, G.; Rosmus, P. *Spectrochim. Acta Part a-Mol. Biomol. Spectrosc.* **1999**, *55*, 447–456.
(32) Jacox, M. E. *J. Phys. Chem. Ref. Data* **2003**, *32*, 123–124.
(33) Eland, J. H. D.; Berkowitz, J. *J. Chem. Phys.* **1977**, *67*, 2782–2787.
(34) Malmqvist, P-Å. *Int. J. Quantum Chem.* **1986**, *30*, 479–494.
(35) Malmqvist, P.-Å.; Roos, B. O. *Chem. Phys. Lett.* **1989**, *155*, 189–194.

JP907351S